Int. J. Plasma Environ. Sci. Technol. 15 (2021) e01003 (13pp)

International Journal of
Plasma Environmental Science and Technology

Regular Paper

DOI: 10.34343/ijpest.2021.15.e01003

Generation of honeycomb discharge assisted by micro-hollow surface dielectric barrier discharge

Richard Cimerman, Karol Hensel*

Division of Environmental Physics, Faculty of Mathematics, Physics and Informatics,
Comenius University, Mlynská Dolina F2, 842 48, Bratislava, Slovakia

* Corresponding author: hensel2@uniba.sk (Karol Hensel)

Received: 19 January 2021
Revised: 20 February 2021
Accepted: 23 February 2021
Published online: 25 February 2021

Abstract

The combination of nonthermal plasma with honeycomb catalysts still represents one of the major challenges in plasma catalysis from the technological point of view. The objective of this paper was to investigate a generation of stable discharge inside the channels of honeycomb catalyst (honeycomb discharge) with the assistance of micro-hollow surface dielectric barrier discharge generated by a perforated ceramic substrate. The surface discharge driven by AC high voltage served as a source of nonthermal plasma and was coupled in series with DC high voltage applied across the honeycomb channels. The honeycomb catalyst was emulated by a bundle of glass capillary tubes that enabled optical emission spectroscopy of the discharge. We investigated the effect of applied AC and DC high voltages, air flow rate and relative humidity on stability and light emission intensity of the honeycomb discharge. We found that generation of honeycomb discharge is positively supported by an increase of air flow rate as well as air relative humidity. A chemical activity of the honeycomb discharge in terms of ozone O_3 production was also briefly examined. The results showed that O_3 concentration increased with an increase of amplitude of both AC and DC high voltages and was found higher for positive than for negative polarity of DC high voltage.

Keywords: Honeycomb catalyst, honeycomb discharge, micro-hollow surface dielectric barrier discharge, capillary discharge, optical emission spectroscopy.

1. Introduction

Plasma catalysis provides a beneficial combination of nonthermal plasma (NTP) with catalysis that has many potential applications. Environmental applications of air and water pollution control [1–5] benefit from the combination of plasma with catalysis as it is often characterised by synergistic effects resulting in enhanced efficiency of the process [6–9]. Nevertheless, plasma catalysis is still facing significant challenges in scalability, energy efficiency, catalyst lifetime, understanding of surface processes, etc. In particular, the combination of NTP with a honeycomb catalyst represents one of the major challenges in plasma catalysis from the technological point of view. The honeycomb catalysts are of great importance in heterogeneous catalysis, as they provide high surface-to-volume ratio, low pressure drop and high mass and heat transfer [10]. Moreover, they are also employed in automotive catalytic converters for exhaust gas cleaning (oxidation of volatile organic compounds VOCs and polycyclic aromatic hydrocarbons PAHs, oxidation of carbon monoxide CO and reduction of nitrogen oxides NO_x). However, their high activity is achieved only at elevated temperatures (> 300 °C) [11, 12] what limits their efficiency especially during winter months. Other drawbacks of automotive catalytic converters are limited lifetime in real conditions due to catalyst poisoning and impossibility of NO_x reduction in strong oxidative environments (i.e. diesel exhaust gases). To overcome these drawbacks, it is necessary to search and investigate new methods, such as their coupling with the NTP. It seems to be a promising idea, as it allows for low-temperature activation of honeycomb catalysts as well as their lifetime enhancement.

However, the combination of the NTP with honeycomb catalysts is still far from a practical use because of the difficulty of stable discharge generation inside their long and narrow channels. Formation of a discharge

in such geometry requires high ignition voltages due to losses of charged particles by interaction with the channel walls [13]. Moreover, the discharge is often unstable and associated with frequent sparking that is undesired due to possible mechanical damage of ceramic honeycomb monolith and also with a respect to some applications [14]. In the recent years, the research in this area has progressed significantly both in the terms of numerical simulations as well as experimental investigations.

For numerical simulations, fluid or particle-in-cell/Monte Carlo collision models have been applied. Jánsky *et al*. simulated a propagation of atmospheric pressure air discharge initiated at a needle anode inside a dielectric capillary tube which emulated a single channel of honeycomb catalyst [15]. They studied the effect of relative permittivity and inner radius of the capillary tube on the discharge structure and dynamics. They found that discharge propagation velocity increases with the decrease of both the tube radius and relative permittivity. In addition, Jánsky *et al*. also performed a comparative study of their results from numerical modelling with the experimental results [16]. They reported a maximum discharge velocity in the tube with radius less than 100 μm which was 3–4 times higher than the velocity obtained without a tube. Hence, a confinement of the discharge in the tube showed significant change of the discharge dynamics, although interaction between the plasma and dielectrics (i.e. catalyst support) was not examined. This interaction was investigated by Zhang and Bogaerts who simulated the discharge propagation in honeycomb-like structures [17]. Their simulations showed that the place where the discharge initiates significantly affects its dynamics as it affects the plasma (i.e. electron) density. They found the discharge being much more enhanced when it initiates at the dielectric surface than at the centre of honeycomb channel (capillary tube). This can be explained by the surface charging process which plays a crucial role in discharge generation and propagation in confined geometry of honeycomb channels. The charging of walls of the channels creates additional electric field along their surface which sums up with applied (external) electric field. The enhanced total electric field pushes the electrons in the direction of discharge propagation resulting in a higher electron density and, thus, discharge enhancement.

In addition to numerical simulations, many experimental investigations have been performed in various geometrical configurations. The first approach utilises a single high voltage (HV) power supply to generate the discharge inside the channels of honeycomb catalyst, i.e. honeycomb discharge [18–23]. Kim used two different systems: the first one was based on inserting the wire electrodes inside the honeycomb channels alternatively powered by HV or grounded, while the second one utilised several smaller elements (slices) of honeycomb catalyst with mesh electrodes placed in parallel between them [22]. Despite promising results for removal of NO_x, the systems were characterised by unstable discharge and frequent sparking. Similar approach was utilised by Nguyen *et al*., Saud *et al*. and Hossain *et al*., who placed a honeycomb catalyst between two perforated electrodes, one powered by AC HV and the other one grounded [23–25]. They reported a generation of stable corona discharge of relatively large volume inside the channels of honeycomb catalyst. Shimizu *et al*. and Rajanikanth *et al*. utilised the dielectric barrier discharge (DBD) of cylindrical geometry inside glass tube equipped with a small honeycomb catalyst [18, 26]. The discharge was generated in a coaxial geometry by application of HV to the electrode placed inside the tube (in its axis), while the other electrode was wrapped around the tube and grounded. Both groups investigated these systems in NO_x removal process, however, the detailed physical characteristics of the generated discharge are missing. Moreover, Ayrault *et al*. and Blin-Simiand *et al*. generated the DBD in a plane-to-plane geometry in a slice of honeycomb catalyst, applied it for 2-heptanone removal process and visualised the discharge propagation perpendicularly to the axis of honeycomb channels using a CCD camera [19, 20]. The authors reported that a development of plasma filaments was randomly distributed inside the honeycomb channels following streamers propagation crossing the channels walls or along their surface. Finally, a regeneration of diesel particulate filter of honeycomb shape was also investigated by Graupner *et al*. using the pulsed discharge generated by a set of electrodes inserted inside the filter channels from both sides [21].

The second approach for generation of honeycomb discharge utilises the idea of the assistance of another discharge [14, 27–35]. In these works, the auxiliary discharge (particularly DBD) was set/coupled in series with a honeycomb monolith. Firstly, the plasma of auxiliary discharge was generated at one nozzle end of the honeycomb monolith. Then, the DC electric field was applied across the monolith, so the generated plasma was extended into the honeycomb channels. It should be noted that in order to simplify the problem, instead of using a real honeycomb ceramic monolith, many authors used a bundle of glass capillary tubes that emulated its shape [14, 27–29, 31, 34, 35]. This enabled visual observation and optical diagnostics of generated honeycomb discharge.

One of the most studied configurations of honeycomb discharge generation utilised a pellet bed DBD [14, 29–31, 35]. Hensel *et al*. and Sato *et al*. generated the honeycomb discharge with the assistance of pellet bed DBD using glass capillary tubes of 20 and 30 mm in length and 1 and 2 mm in diameter and performed its electrical and optical characterisation [14, 29, 31]. Takashima *et al*. studied the effect of air humidity and temperature on honeycomb discharge generation and properties and found their positive effect on discharge stability [35]. The chemical activity of the honeycomb discharge assisted by pellet bed DBD was investigated by Sato & Mizuno [30]. They studied NO_x removal in the selective catalytic reduction (SCR) process using Fe-zeolite-supported honeycomb catalyst and NH_3 as a reduction agent. In addition to a pellet bed DBD, various types of surface dielectric barrier discharges (SDBDs) were also employed as auxiliary discharges for honeycomb discharge generation [27, 28, 36]. Hensel *et al*. used a diffuse coplanar surface barrier discharge (DCSBD) with both electrodes embedded inside the Al_2O_3 ceramics [28, 36]. Mizuno utilised a micro-hollow SDBD generated by a perforated ceramic substrate consisting of one electrode printed on the ceramic surface and the other one embedded inside the ceramic [27]. Furthermore, Takashima *et al*. reported honeycomb discharge generation by using two ceramic substrates generating the micro-hollow SDBD placed at the opposite nozzle ends of a bundle of glass capillary tubes [35]. In addition, the applications of honeycomb discharge generated with the assistance of SDBDs have been studied, too. Seiyama *et al*. and Mizuno & Takashima studied the utilisation of honeycomb discharge for regeneration of diesel particulate filter of honeycomb shape [33, 34].

The works mentioned above demonstrated and described the possibility of plasma generation inside the honeycomb catalyst by using various discharge geometries. The authors demonstrated that a common system of plasma and honeycomb catalyst can be successfully used, although there are still issues that must be resolved and improved. One of them is that the total volume of generated plasma is often unknown, i.e. it is not clear whether the plasma can be generated inside every channel of honeycomb catalyst or only inside some of them. Another uncertainty comes with a lack of data of discharge stability: many authors did not clearly report whether the honeycomb discharge was operated in a stable streamer mode (regime) or in an unstable spark mode, what is crucial in respect to eventual applications. In addition, many studies focused only on a particular application of the honeycomb discharge without presenting detailed electrical and optical characterisation of the generated discharge. Therefore, underlying mechanisms of honeycomb discharge generation are still not yet fully resolved and require further research.

The objective of this paper is to build on our previous works [14, 28, 29, 31, 36] and the works of other authors from recent years and to further investigate alternative methods of honeycomb discharge generation and its basic electrical and optical properties. More specifically, the honeycomb discharge generation was investigated with an assistance of the micro-hollow SDBD generated by a perforated ceramic substrate in configuration with the air-exposed electrode. The honeycomb shape was emulated by a bundle of glass capillary tubes. The effects of the applied voltage, air relative humidity and air flow rate were studied on electrical and optical characteristics of generated discharge. Moreover, the effect of the polarity of DC HV applied across the capillary tubes was investigated on quality (stability) and homogeneity of the honeycomb discharge. Finally, plasma chemical effects of the discharge were briefly examined and evaluated in terms of ozone O_3 production.

A substitution of a ceramic honeycomb monolith by a glass capillary tubes was made to visually observe the discharge inside the tubes and to perform its optical diagnostics. A choice of a material affects the electrical and optical properties of the discharge as well as the chemical effects of the discharge, therefore the results obtained with glass capillary tubes may be slightly different that would be those in a ceramic honeycomb monolith. This is a very important issue to consider with respect to eventual applications and system optimisation, although in the presented study and at this early stage of the research this issue has not been explicitly addressed.

2. Methods

The experimental setup is depicted in Fig. 1 (a). The micro-hollow SDBD served as an auxiliary (assisting) discharge and was generated by a perforated ceramic substrate (KD-EB2B10, Kyocera) with the dimensions of 50 × 50 × 1 mm and perforated by 170 holes with an inner diameter of 1.5 mm (Fig. 1 (b, c)). The electrodes were made of Ni/Au alloy; one was embedded inside the ceramic and the other one was printed on the ceramic surface (air-exposed electrode).

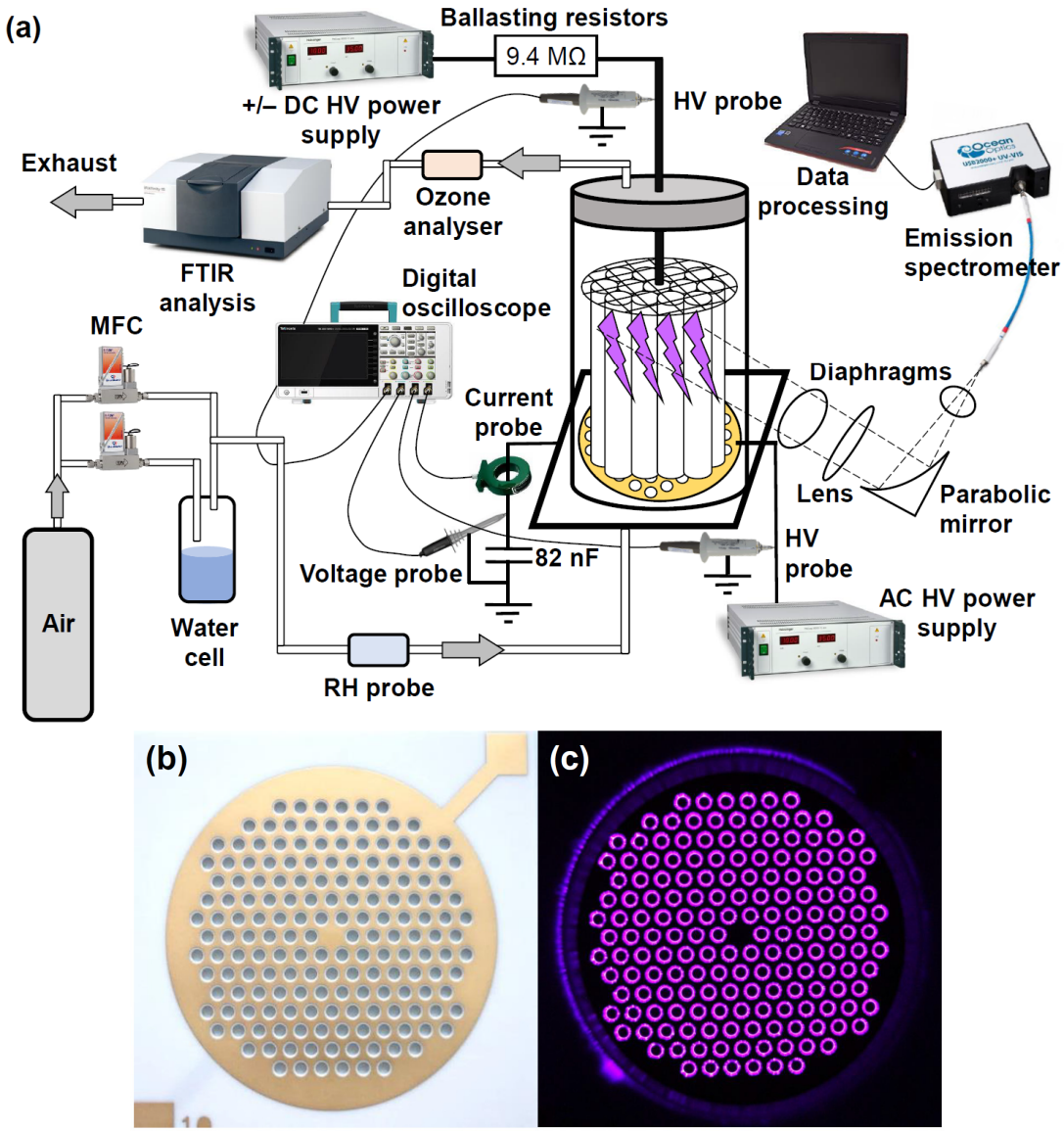

Fig. 1. (a) Experimental setup and photographs of the (b) perforated ceramic substrate and (c) micro-hollow SDBD [Exposure time 3 s, f/5.6, ISO 400].

The substrate was powered by AC HV power supply consisting of a function generator (GwInstek SFG-1013), signal amplifier (Omnitronic PAP-350) and high voltage transformer. The micro-hollow SDBD was generated by applying AC HV to the air-exposed electrode, while the other one was grounded. The maximum amplitude of the applied voltage was 3–6 kV (i.e. 6–12 kV_{pk-pk}) and a frequency was 1 kHz. The bundle of glass capillary tubes made of borosilicate glass was placed inside the quartz glass tube perpendicularly to the ceramic substrate on the top of air-exposed electrode, while a metal mesh serving as a remote electrode was placed on the top of capillary tubes and connected to a DC HV power supply (Technix SR20-R-1200) through ballasting resistors (9.4 MΩ). The bundle consisted of 48 capillary tubes (Ø 2.8 mm (i. d.) × Ø 4 mm (o. d.) × 20 mm (length)). The waveforms of the applied AC and DC voltages were measured by HV probes (Tektronix P6015A) and the discharge current was measured by a current probe (Pearson Electronics 2877) connected to a digital oscilloscope (Tektronix TBS2000). The power consumption of the micro-hollow SDBD was evaluated using the Lissajous figure method with an 82 nF capacitor and a voltage probe (Tektronix P2220). The power consumption corresponding to pulsed current component of the honeycomb discharge was estimated from the recorded current waveforms by calculating an area enclosed by current pulses, each of them sampled with a sufficient number of data points. An optical emission spectroscopy (OES) system consisted of dual-fibre optic spectrometer (Ocean Optics SD2000), optic fibre, two diaphragms, parabolic mirror and cylindrical lens. The OES system was adjusted to collect light signal from a plane perpendicular to the axis of

capillary tubes approximately 3 mm below the top of the tubes. This enabled to collect light emitted by the honeycomb discharge formed in several capillary tubes integrated over 8 s. Photographs of the discharge were taken with a digital camera (Sony Alpha DSLR-A230) with manually adjustable aperture and exposure. Dry synthetic air (purity 5.0) supplied from a pressure tank was used as the carrier gas and its flow rate (0.5, 1 and 2.4 L min^{-1}) was controlled by mass flow controllers (MFC) (Bronkhorst El-Flow Prestige FG-201CV). The air was alternatively enriched with water vapours by passing it through a water cell. The air relative humidity (RH) was monitored (0–80%) by an electrochemical probe (Arduino). Then the air was led into the reactor from the bottom side of the ceramic substrate, it passed through the perforated substrate, then capillary tubes and, finally, it exited the reactor. Chemical effects induced by the discharge in the gas phase, i.e. production of ozone O_3, nitrous oxide N_2O and nitric acid HNO_3, were evaluated by means of FTIR spectroscopy (Shimadzu IR-Affinity 1S) using a 10 cm gas cell equipped with CaF_2 windows. Ozone production was also evaluated by a homemade ozone analyser based on UV absorption at 254 nm.

3. Results and discussion

3.1 Discharge characterisation

Fig. 2 shows side and perspective view of the reactor with ceramic substrate and bundle of glass capillary tubes in different conditions: (a) without any applied HV; (b) with only AC HV applied, (c) with both AC and DC HVs applied, and (d) with only DC HV applied. When only AC HV was used, the light was emitted only by the auxiliary micro-hollow SDBD at the bottom of the reactor (Fig. 2 (b)). When both AC and DC HVs were applied, the streamers occurred and propagated inside the capillary tubes and formed homogeneous honeycomb discharge (Fig. 2 (c)). When only DC HV without the assistance of the surface discharge was applied, the honeycomb discharge did not form. Light was emitted only by a corona discharge generated in the vicinity of the DC powered mesh electrode (Fig. 2 (d)). Based on these observations we might conclude that generation of stable and homogeneous streamer discharge inside glass capillary tubes benefits from an assistance of the auxiliary micro-hollow SDBD and application of DC HV applied across the tubes. The mechanism governing honeycomb discharge generation can be explained by a superposition of the AC powered surface discharge and the DC powered corona discharge. The first one serves as an ioniser producing charged particles while the latter one produces and maintains ionic wind toward the DC electrode, thus forming streamers inside the capillary tubes [14].

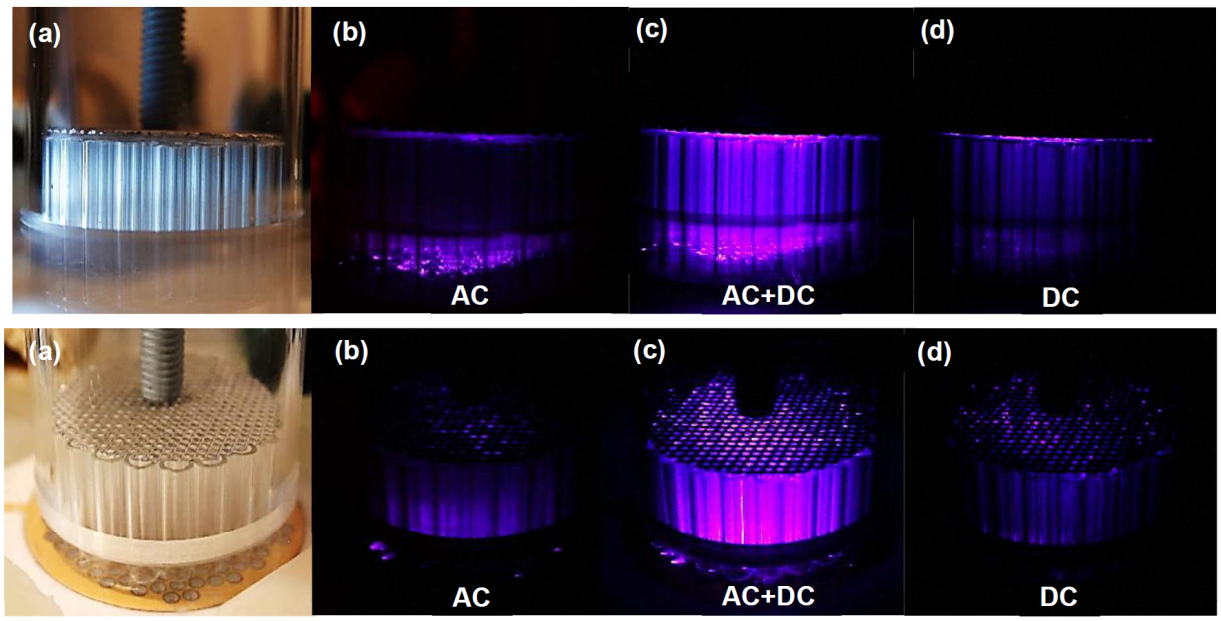

Fig. 2. The ceramic substrate with glass capillary tubes – side and perspective view: (a) without discharge; (b) with applied AC HV only (amplitude 4 kV at 1 kHz); (c) with applied both AC and DC HVs (4 kV at 1 kHz; +14 kV, respectively); (d) with applied DC HV only (+14 kV) (RH ~ 60%; 2.4 L min^{-1}) [Exposure time 8 s, f/5.6, ISO 400].

Fig. 3 shows a comparison of voltage and current waveforms of micro-hollow SDBD and honeycomb discharge for positive polarity of DC HV. The waveform of micro-hollow SDBD contains a typical DBD current record (Fig. 3 (a)). However, when a positive DC HV was applied to the remote mesh electrode, relatively high current pulses with amplitudes up to 200 mA occurred in the current waveform (Fig. 3 (b)). These pulses were attributed to the honeycomb discharge formed inside the capillary tubes. When positive DC HV was used, the current pulses of honeycomb discharge appeared only during the negative half-period of the applied AC HV. On the contrary, with negative DC HV the pulses were observed only during the positive half-period of the applied AC HV. Explanation can be given as follows: the pulses, i.e. honeycomb discharge, appeared when an electric field strength applied across the capillary tubes reached the highest values. In a case of positive DC HV, it happens at the peak voltage during the negative half-period of the applied AC HV, and vice-versa. Thus, the voltage across the capillary tubes was changing in time with a frequency of the AC HV (e.g. for DC amplitude +16 kV and AC amplitude 4 kV, the net voltage applied across the capillary tubes changed in a range of 12–20 kV). The DC corona discharge that developed within this range of the applied voltages passed through several discharge modes, some of them being pulsed (streamer mode corresponding to current pulses visible on the waveform in Fig. 3 (b)), other being unipolar (glow mode). The transition between the modes happened during each period of the applied AC HV. To evaluate the honeycomb discharge power consisting of the power of SDBD and the power induced by DC HV, one must measure both pulsed and unipolar (continuous) components of the discharge current. Although we did not measure the unipolar component of the current, we tried at least to estimate the power consumption corresponding to pulsed current component from the recorded current waveforms. The power was found higher for positive than negative polarity of DC HV and the maximum values were in a range of 0.4–0.6 W (+DC, RH 60%, 2.4 L min^{-1}). For a comparison, the power of micro-hollow SDBD was in a range of 0.3–4.3 W depending on the amplitude of AC HV in a range of 3–6 kV, respectively. Therefore, we can hypothesize that the total power of honeycomb discharge is probably not higher than 10 W.

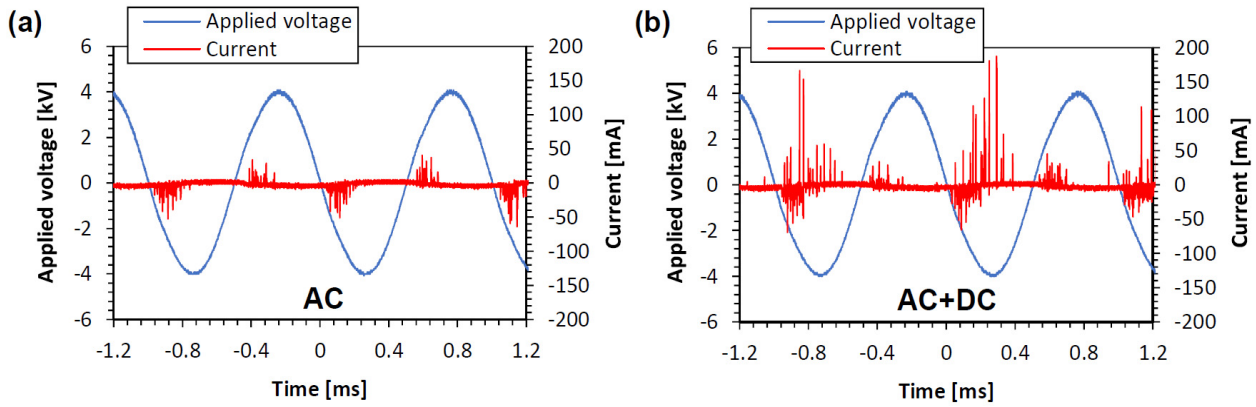

Fig. 3. Voltage and current waveforms of (a) micro-hollow SDBD (AC HV amplitude 4 kV at 1 kHz; ~ 1.8 W) in comparison with (b) honeycomb discharge (AC HV amplitude 4 kV at 1 kHz; DC HV +16 kV; RH ~ 60%; 2.4 L min^{-1}).

3.2 The effect of the air flow rate

Evaluation of the honeycomb discharge quality (stability, homogeneity) was performed by measuring its light emission intensity in various conditions. In the measured emission spectra, N_2 second positive system was dominant. As the capillary tubes were made of borosilicate glass, strong attenuation of the light emission intensity occurred below 350 nm. For this reason, the discharge emission intensity was further evaluated based on the 0–1 spectral band (357 nm) of N_2 second positive system instead of 0–0 spectral band (337 nm).

In general, a higher signal of integrated emission intensity corresponds to higher number of stable discharges maintained in the streamer discharge mode. Possible instability of the discharge is associated with a transition from the streamer to the spark mode, what is usually undesirable. The emission intensity is also a measure of discharge activity, *i.e.* concentration of reactive species generated by the discharge. Hensel investigated the configuration with an auxiliary pellet bed DBD and reported an excessive sparking when operating honeycomb discharge in dry gas mixtures [14]. He further reported that the streamer-like behaviour of the discharge was

supported with an increase of the gas humidity, but details of discharge behaviour with a gas humidity were not examined. Therefore, we investigated the effect of air RH on stability and quality of honeycomb discharge. Besides, the effects of air flow rate and polarity of applied DC HV were also examined.

Fig. 4 shows light emission intensity of the honeycomb discharge as a function of amplitude of applied DC HV (11–16 kV) for various air flow rates and both DC HV polarities. When amplitude of AC HV was set to 4 kV, the honeycomb discharge started to occur for DC HV amplitudes in a range of 12–14 kV (i.e. ignition voltage). Then, an average ignition electric field strength for honeycomb discharge generation was found to be in a range of 8–9 kV/cm which is slightly lower than 10 kV/cm reported by Sato *et al*. who used the assistance of pellet bed DBD [29]. The maximum amplitude of DC HV (i.e. sparking voltage) was found to be in a range of 16–17 kV. When this value was exceeded, a permanent sparking inside the capillary tubes occurred. From the ignition to the sparking voltage (i.e. in a range of 12–16 kV), the discharge was maintained in a stable streamer discharge mode. Fig. 4 further shows an increase of light emission intensity of the honeycomb discharge with an increase of air flow rate. Thus, the air flow rate positively supported the honeycomb discharge generation and this effect was stronger for positive polarity of DC HV.

The air residence time inside the capillary tubes was 0.74, 0.37 and 0.15 s corresponding to air flow rate of 0.5, 1 and 2.4 L min^{-1}, respectively. Due to different time scales of the mechanisms of discharge formation (ps to μs) and gas flow dynamics (ms to s), the gas flow cannot directly affect an ignition and propagation of individual discharge filaments [37]. However, it can affect the conditions prior to the ignition by changing the level of pre-ionisation what may subsequently affect the ignition voltage or peak current [37]. Indeed, the effect of gas flow rate on discharge dynamics is particularly important for plasma jets [38–40]. In our configuration, the air flow passed first through the perforated ceramic substrate and then through the capillary tubes. Thus, the air flow enhanced a transport of charged particles from the surface "seeding" discharge into the tubes. Consequently, a higher air flow rate resulted in higher number of seeding particles inside the capillary tubes what enhanced a honeycomb discharge generation and its emission intensity. The effect of the air flow on honeycomb discharge was also studied by Nguyen *et al*. and they reported an increase in the discharge current with an increase of the air flow rate [23]. Similarly, Saud *et al*. reported a gas flow rate as one of the key parameters affecting the honeycomb discharge performance [24].

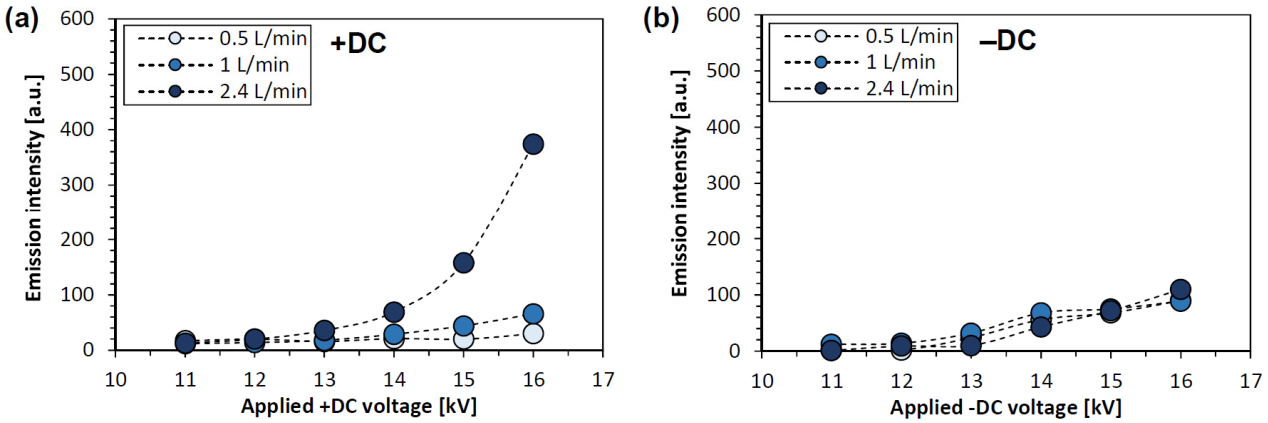

Fig. 4. Emission intensity of the honeycomb discharge as a function of applied (a) positive and (b) negative DC HV for various air flow rates (AC HV amplitude 4 kV at 1 kHz; RH ~ 55%).

3.3 The effect of the air relative humidity

In addition to the air flow, the positive effect on the honeycomb discharge quality was also observed with the increase of the air RH. When dry air was used as a carrier gas, the auxiliary micro-hollow SDBD showed the highest stability and light emission intensity. On the contrary, in dry air the honeycomb discharge did not form at all regardless of air flow rate and amplitude and polarity of the DC HV. When the air RH was increased, the honeycomb discharge in capillary tubes started to form and its higher emission intensity was always observed when using positive DC HV. On the contrary, when negative DC HV was applied, the honeycomb discharge was less stable and sparking voltage was found to be slightly lower (~15–16 kV). Therefore, we hypothesise, the positive DC HV caused that negatively charged electrons produced by the micro-hollow SDBD were

intensively driven into the capillary tubes what in turn resulted in more efficient discharge formation inside them and, thus, higher discharge emission intensity. The effect of polarity of DC HV was also tested by Hensel using an auxiliary pellet bed DBD [14]. Even though he did not compare an emission intensity of the discharge for both DC HV polarities, he observed a bigger range between ignition and sparking voltage for stable discharge operation without sparking for negative polarity. However, this effect was not observed in our experiment.

Fig. 5 shows light emission intensity of the honeycomb discharge as a function of amplitude of DC HV and various air RHs. For positive DC HV, the emission intensity increased with an increase of air RH from 0 to 60% and subsequently with further increase of air RH to 80%, it decreased below values with air RH of 40 and 60% (Fig. 5 (a)). On the contrary, when negative DC HV was used, the emission intensity monotonously increased with air RH from 0 to 80% (Fig. 5 (b)). However, the overall emission intensity of the discharge was lower with negative than positive DC HV. In general, the humidity has a substantial effect on electric discharges as it affects a distribution of electric field [41, 42], a mobility of charge carriers [43], plasma chemistry [44], etc. Its exact effect also depends on working conditions (composition of gas mixture, gas pressure, etc.) and the type of electric discharge. Therefore, the humidity effect is generally very complex and must be investigated carefully with respect to other working conditions. In our case we hypothesise that enhancement of honeycomb discharge formation with increasing air RH may be attributed to an enhancement of surface electrical conductivity of glass capillary tubes. As already mentioned, when a discharge is initiated along the capillary tubes surface, its propagation is enhanced due to surface charging phenomenon [17]. The discharge propagation along the capillary tubes surface could be further enhanced as a result of enhanced surface electrical conductivity provided by water adsorption onto capillary tubes surface. Such explanation was also given by Nguyen *et al*. [23]. Our hypothesis is further supported by findings of Falkenstein and Coogan who investigated a behaviour of DBD microdischarges in humid air mixtures [45]. They reported that a dominant effect of air humidity on DBD is not the electronegativity of water molecules, but rather its influence on surface resistance of the dielectric. In the presence of water vapours in air, the water molecules can adsorb onto dielectric, thus reduce surface dielectric resistance, and increase the effective dielectric capacity. Consequently, the authors reported that the discharge spread over a wider area when humid air was used. In addition to the effect of water adsorption, the type of material of capillary tubes may also affect the discharge propagation. As it is well known, the use of various materials in the reactor can induce substantial changes in equivalent electrical circuits, what may further influence the discharge characteristics, formation, and propagation and also its chemical activity [46]. Thus, this point must be considered especially in case when glass capillary tubes are replaced with other materials, for example ceramic honeycomb monolith.

An influence of air RH on honeycomb discharge generation assisted by pellet bed DBD was also studied by Takashima *et al*. [35]. They also reported a positive role of air humidity on the discharge generation and stability: below air RH of 30%, the discharge did not form, while above 30%, a stable DC voltage region increased with an increase of air humidity regardless of DC HV polarity. This observation approximately corresponds to our findings.

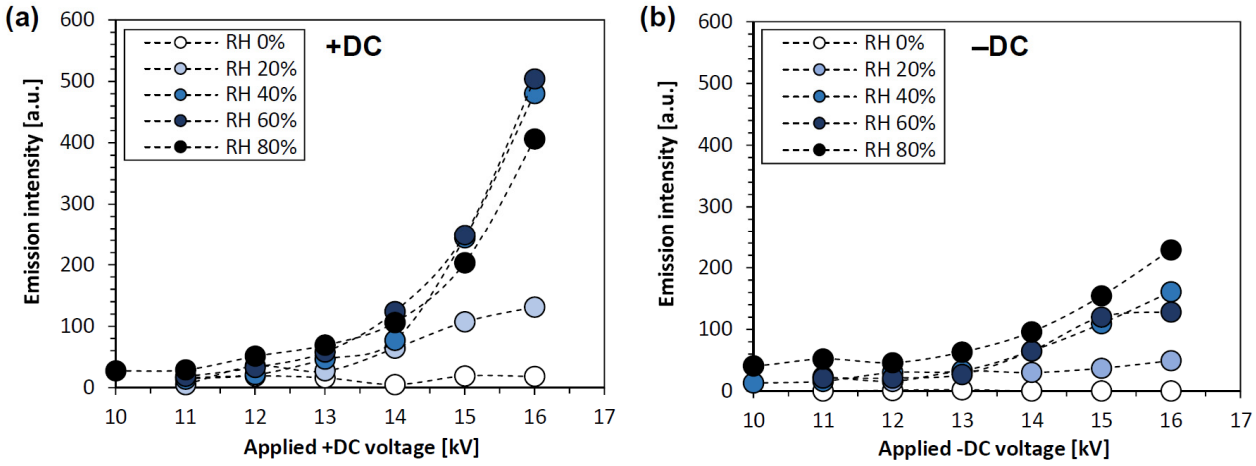

Fig. 5. Emission intensity of the honeycomb discharge as a function of applied (a) positive and (b) negative DC HV at various air RHs (AC HV amplitude 4 kV at 1 kHz; 2.4 L min^{-1}).

3.4 Chemical activity

A brief evaluation of honeycomb discharge chemical activity in terms of various reactive species production (O_3, N_2O, NO, NO_2, HNO_3) was carried out by FTIR spectroscopy. Fig. 6 shows the infrared absorption spectrum of gaseous products of the honeycomb discharge in air with RH of 40%. In the spectrum, we positively identified ozone O_3 (1055 and 2125 cm^{-1}), nitrous oxide N_2O (2236 cm^{-1}) and nitric acid HNO_3 (1325 and 1711 cm^{-1}) whose concentrations increased with an increase of amplitudes of both AC and DC HVs and reached maximum levels of approx. 320 ppm, 10 ppm and 40 ppm, respectively. The O_3 is formed by a reaction of O radicals with O_2 molecules, whereas N_2O production depends on a presence of nitrogen and oxygen species, such as N_2 (A), $N(^2D)$, N and $O(^1D)$ [46–51]. While O_3 and N_2O represent basic gaseous products of atmospheric pressure air electric discharges in general, HNO_3 represents the highest oxidation level of nitrogen oxides NO_x produced by the discharge. Basically, it is formed in a presence of water molecules in air via gradual oxidation of NO_x by O, OH and HO_2 radicals or eventually by H_2O_2 [53]. On the other hand, nitric oxide NO and nitrogen dioxide NO_2 were not detected in the spectra at all implying their fast oxidation towards HNO_3.

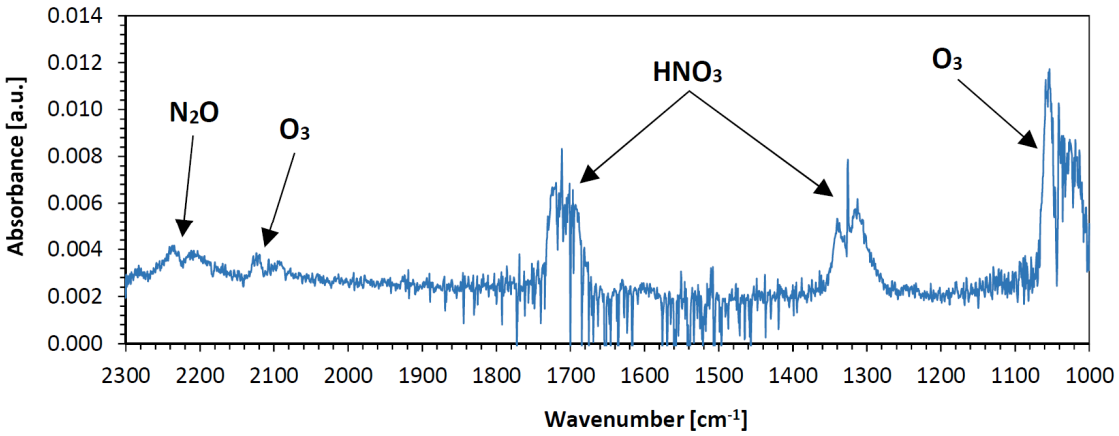

Fig. 6. Infrared absorption spectrum of gaseous products of the honeycomb discharge in air (AC HV amplitude 5 kV at 1 kHz; ~ 2.9 W; DC +17 kV; RH ~ 40%; 2.4 L min^{-1}).

A production of O_3 was further evaluated by means of absorption analyser (at 254 nm) as a function of applied AC and positive DC HV amplitudes and air RHs. Fig. 7 compares O_3 concentration obtained with various discharge regimes: (a) when AC HV was applied (amplitude 3–5 kV at 1 kHz) without application of DC HV (0 kV), the O_3 production relates to the auxiliary micro-hollow SDBD; (b) when both AC and positive DC HV were applied (amplitude 3–5 kV at 1 kHz, 13–17 kV, respectively), the O_3 production relates to a combination of surface and honeycomb discharge; (c) when only positive DC HV was applied (13–17 kV), the O_3 production relates to a corona discharge generated in a vicinity of the remote mesh electrode. As it is generally known, the O_3 production decreases with an increase of air RH. It can be attributed to higher consumption of O radicals via reaction with H_2O molecules or HO_2 and OH radicals [49, 53]. As O radicals are essential for O_3 production, their loss leads to lower O_3 production. Further, a decomposition of O_3 is also different for dry and humid air: while in dry air the main O_3 decomposition pathway is governed by NO, in humid air it is primarily by OH radicals [44]. However, our results showed that for AC HV amplitude of 5 kV, the O_3 production was slightly higher at RH of 60% than at RH of 40% (Fig. 7). It is due to the fact described in section 3.3 that at higher air RH, the honeycomb discharge is more enhanced, stable, and intense, leading to higher O_3 production. Note that the error bars in Fig. 7 represent standard deviations of the data.

Further, O_3 production increased with amplitude of DC HV and it was always higher when both AC and DC HVs were applied than when AC HV was used alone. Indeed, the honeycomb discharge was formed inside the capillary tubes only upon application of both AC and DC HVs. The honeycomb discharge is characterised by a higher chemical activity than auxiliary micro-hollow SDBD alone due to a larger volume of generated plasma and, thus, higher O_3 production. A comparison of O_3 production by honeycomb discharge for both DC HV polarities was also examined and showed a higher O_3 production for positive polarity. Pekárek and also Abdel-Salam *et al*. studied the effect of polarity of DC streamer corona discharge on O_3 production and reported higher O_3 concentration for positive polarity [54, 55]. The same effect was also experimentally investigated

by Brandvold *et al*. and by numerical modelling by Chen and Davidson, however, they reported the opposite results with higher O_3 production for negative polarity [56, 57]. Therefore, the dependence of O_3 production on polarity of applied DC HV is not straightforward as it generally depends on several factors, including discharge current, size of plasma region, distribution and density of electrons, gas temperature and gas flow rate [54–56, 58]. Moreover, the discharge mode (regime) seems to be one of the critical parameters determining O_3 production by positive and negative DC corona discharges: in a glow mode, a negative corona discharge produces more O_3 than a positive corona discharge. The situation is reversed in a streamer discharge mode, when higher O_3 production was reported with a positive corona discharge [60]. This fact can explain the observed higher O_3 production by using positive DC HV, as the honeycomb discharge in our study was maintained in a stable streamer mode.

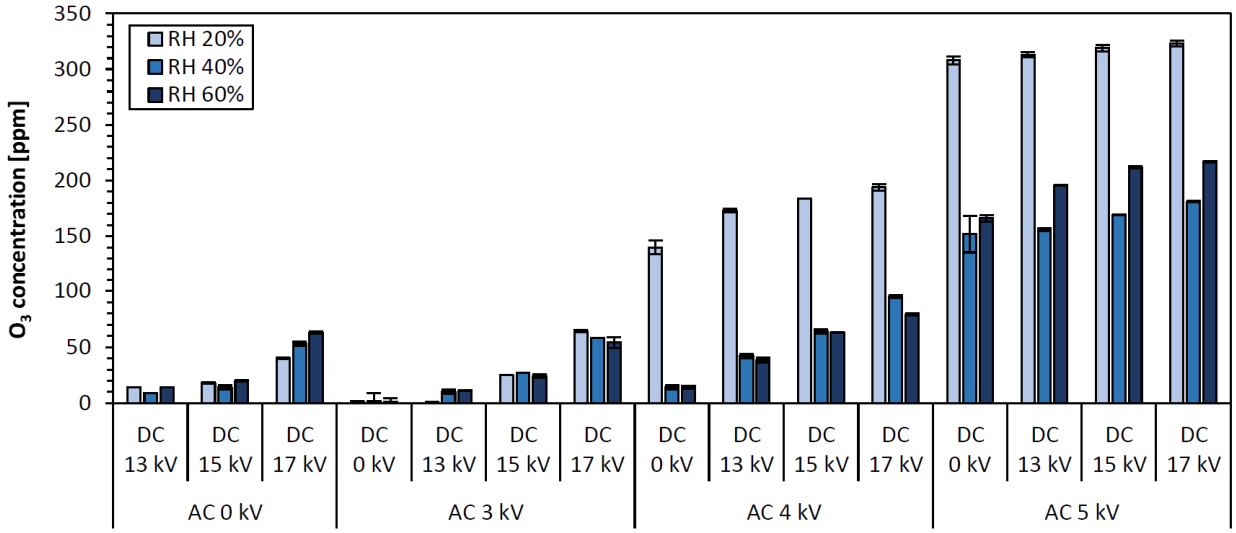

Fig. 7. Concentration of O_3 produced by auxiliary micro-hollow SDBD (when DC HV = 0 kV) and honeycomb discharge as a function of various combinations of applied AC and positive DC HV amplitudes and various air RHs (2.4 L min^{-1}).

4. Conclusion

The combination of nonthermal plasma with honeycomb catalysts is a very promising method for the environmental applications particularly for gas cleaning applications. However, a coupling of the plasma with honeycomb catalysts still represents one of the major challenges in plasma catalysis. The presented research was built on our previous works and the works of other authors and its objective was to further investigate electrical, optical, and chemical properties of honeycomb discharge and to find its optimal operating conditions. Our results demonstrated that generation and sustaining a stable discharge inside the honeycomb catalyst emulated by a bundle of glass capillary tubes is possible with an assistance of surface barrier discharge coupled in series with DC electric field applied across the tubes. The auxiliary micro-hollow surface dielectric barrier discharge (SDBD) was generated by a perforated ceramic substrate. A bundle of capillary tubes was placed perpendicularly on the ceramic substrate and DC high voltage (HV) was applied to a remote mesh electrode placed at the other nozzle ends of the tubes. Then, DC electric field extended plasma streamers formed by the auxiliary micro-hollow SDBD into the capillary tubes what resulted in honeycomb discharge generation.

The results showed that the honeycomb discharge did not form in dry air. Its stability as well as light emission intensity was positively supported by an increase of both air flow rate and air relative humidity. We consider that air flow supported a transport of charged particles from the surface barrier discharge into the capillary tubes and, thus, pre-ionisation processes, while humidity supported an enhancement of surface electrical conductivity of the glass capillary tubes and, thus, honeycomb discharge generation. Furthermore, light emission intensity of the discharge was higher for positive DC HV when comparing to negative DC HV. A brief evaluation of chemical activity of the honeycomb discharge in terms of particularly ozone O_3 production was also carried out. It showed that O_3 concentration increased with an increase of amplitude of both AC and DC HVs and was higher for positive than for negative polarity of DC HV.

Finally, we may conclude that our work may serve as a good starting point for future experimental investigations in real ceramic monoliths. Here the generated plasma pattern and its chemical activity can be slightly different than the plasma in the glass capillary tubes. Under a proper design the plasma activity can be further enhanced and if successfully scaled-up it may become of a huge interest with a respect to the practical applications.

Acknowledgment

This research was funded by Slovak Research and Development Agency grant APVV-17-0382, Slovak Grant Agency VEGA 1/0822/21 and Comenius University grant UK/222/2020.

References

[1] Magureanu M., Bradu C., and Parvulescu V. I., Plasma processes for the treatment of water contaminated with harmful organic compounds, *J. Phys. D. Appl. Phys*., Vol. 51 (31), pp. 313002, 2018.
[2] Parvulescu V. I., Magureanu M., and Lukeš P., Plasma Chemistry and Catalysis in Gases and Liquids. Wiley-VCH Verlag GmbH and Co., 2012.
[3] Van Durme J., Dewulf J., Leys C., and Van Langenhove H., Combining non-thermal plasma with heterogeneous catalysis in waste gas treatment: A review, *Appl. Catal. B Environ*., Vol. 78 (3–4), pp. 324–333, 2008.
[4] Vandenbroucke A. M., Morent R., De Geyter N., and Leys C., Non-thermal plasmas for non-catalytic and catalytic VOC abatement, *J. Hazard. Mater*., Vol. 195, pp. 30–54, 2011.
[5] Whitehead J. C., Plasma catalysis: A solution for environmental problems, *Pure Appl. Chem*., Vol. 82 (6), pp. 1329–1336, 2010.
[6] Whitehead J. C., Plasma-catalysis: The known knowns, the known unknowns and the unknown unknowns, *J. Phys. D. Appl. Phys*., Vol. 49 (24), pp. 243001, 2016.
[7] Mei D., Zhu X., Wu C., Ashford B., Williams P. T., and Tu X., Plasma-photocatalytic conversion of CO_2 at low temperatures: Understanding the synergistic effect of plasma-catalysis, *Appl. Catal. B Environ*., Vol. 182, pp. 525–532, 2016.
[8] Tu X. and Whitehead J. C., Plasma-catalytic dry reforming of methane in an atmospheric dielectric barrier discharge: Understanding the synergistic effect at low temperature, *Appl. Catal. B Environ*., Vol. 125, pp. 439–448, 2012.
[9] Bogaerts A., Tu, X., Whitehead, J. C., Centi, G., Lefferts, L., Guaitella, O., Azzolina-Jury, F., Kim, H.-H., Murphy, A. B., Schneider, W. F., Nozaki, T., Hicks, J. C., Rousseau, A., Thevenet, F., Khacef, A., and Carreon, M., The 2020 plasma catalysis roadmap, *J. Phys. D. Appl. Phys*., Vol. 53 (44), pp. 443001, 2020.
[10] Williams J. L., Monolith structures, materials, properties and uses, *Catal. Today*, Vol. 69, pp. 3–9, 2001.
[11] Hagen J., Industrial Catalysis: A Practical Approach. Wiley-VCH Verlag GmbH and Co., 2006.
[12] Ertl G., Knozinger H., and Weitkamp J., Environmental catalysis. Wiley-VCH Verlag GmbH and Co., 2005.
[13] Cheng H., Lu X., and Liu D., The Effect of Tube Diameter on an Atmospheric-Pressure Micro-Plasma Jet, *Plasma Process. Polym*., Vol. 12, pp. 1343–1347, 2015.
[14] Hensel K., Microdischarges in ceramic foams and honeycombs, *Eur. Phys. J. D*, Vol. 54 (2), pp. 141–148, 2009.
[15] Jánský J., Tholin F., Bonaventura Z., and Bourdon A., Simulation of the discharge propagation in a capillary glass tube in air at atmospheric pressure, *J. Phys. D. Appl. Phys*., Vol. 43 (39), pp. 173–177, 2010.
[16] Jánský J., Le Delliou P., Tholin F., Tardiveau P., Bourdon A., and Pasquiers S., Experimental and numerical study of the propagation of a discharge in a capillary tube in air at atmospheric pressure, *J. Phys. D. Appl. Phys*., Vol. 44 (33), pp. 335201, 2011.
[17] Zhang Q. Z. and Bogaerts A., Plasma streamer propagation in structured catalysts, *Plasma Sources Sci. Technol*., Vol. 27 (10), pp. 105013, 2018.
[18] Rajanikanth B. S., Kumar P. K. S., and Ravi V., Non-Conventional Plasma Assisted Catalysts for Diesel Exhaust Treatment: A Case Study, *Plasma Sci. Technol*., Vol. 4 (1), pp. 1119–1126, 2002.
[19] Ayrault C., Barrault, J., Blin-Simiand, N., Jorand, F., Pasquiers, S., Rousseau, A., Tatibouët, J.M., Oxidation of 2-heptanone in air by a DBD-type plasma generated within a honeycomb monolith supported Pt-based catalyst, *Catal. Today*, Vol. 89 (1–2), pp. 75–81, 2004.
[20] Blin-Simiand N., Tardiveau P., Risacher A., Jorand F., and Pasquiers S., Removal of 2-heptanone by dielectric barrier discharges - The effect of a catalyst support, *Plasma Process. Polym*., Vol. 2 (3), pp. 256–262, 2005.

[21] Graupner K., et al., Pulsed discharge regeneration of diesel particulate filters, *Plasma Chem. Plasma Process*., Vol. 33 (2), pp. 467–477, 2013.
[22] Kim H.-H., Application of Non-thermal Plasma in Environmental Protection, Ph.D. Thesis, Toyohashi University of Technology, Toyohashi, Japan, 2000.
[23] Nguyen D. B., Shirjana S., Hossain M. M., Heo I., and Mok Y. S., Effective generation of atmospheric pressure plasma in a sandwich-type honeycomb monolith reactor by humidity control, *Chem. Eng. J.*, Vol. 401, pp. 125970, 2020.
[24] Saud S., Nguyen, D.B., Bhattarai R.M., Matyakubov N., Heo, I., Kim, S.J., Kim, Y.J., Lee, J.H., Mok, Y.S., Dependence of humidified air plasma discharge performance in commercial honeycomb monoliths on the configuration and key parameters of the reactor, *J. Hazard. Mater*., Vol. 404, pp. 124024, 2021.
[25] Hossain M., Mok, Y.S., Nguyen, D.B., Kim, S.J., Kim, Y.J., Lee, J.H., Heo, I., Nonthermal plasma in practical-scale honeycomb catalysts for the removal of toluene, *J. Hazard. Mater*., Vol. 404, pp. 123958, 2021.
[26] Shimizu K., Hirano T., and Oda T., Effect of water vapor and hydrocarbons in removing NO_x by using nonthermal plasma and catalyst, *IEEE Trans. Ind. Appl.*, Vol. 37 (2), pp. 464–471, 2001.
[27] Mizuno A., Generation of non-thermal plasma combined with catalysts and their application in environmental technology, *Catal. Today*, Vol. 211, pp. 2–8, 2013.
[28] Hensel K., Janda M., and Ráheľ J., Generation of discharges inside the honeycomb monolith assisted by diffuse coplanar surface barrier discharge, *19th International Symposium on Plasma Chemistry*, Bochum, 2009.
[29] Sato S., Hensel K., Hayashi H., Takashima K., and Mizuno A., Honeycomb discharge for diesel exhaust cleaning, *J. Electrostat*., Vol. 67 (2–3), pp. 77–83, 2009.
[30] Sato S. and Mizuno A., NO_x removal of simulated diesel exhaust with honeycomb discharge, *Int. J. Plasma Environ. Sci. Technol*., Vol. 4 (1), pp. 18–23, 2010.
[31] Hensel K., Sato S., and Mizuno A., Sliding discharge inside glass capillaries, IEEE Trans. Plasma Sci., Vol. 36, pp. 1282–1283, 2008.
[32] Hayashi H., Sakiyama D., Takashima K., and Mizuno A., Collection of diesel exhaust particles using electrostatic charging prior to DPF and regeneration of DPF using sliding discharge, *Int. J. Plasma Environ. Sci. Technol*., Vol. 6 (2), pp. 160–165, 2012.
[33] Seiyama R., Yamaji T., Hayashi H., Takashima K., and Mizuno A., Regeneration of diesel particulate filter using sliding discharge, *IEEE Ind. Appl. Soc. Annu. Meet*., 2013.
[34] Mizuno A. and Takashima K., Non-thermal plasma combined with catalysts for environmental technology, *HAKONE XV*, pp. 34–37, 2016.
[35] Takashima K., et al., Honeycomb discharge generated with a single high voltage power supply for activating catalyst, *Int. J. Plasma Environ. Sci. Technol*., Vol. 7 (2), pp. 142–147, 2013.
[36] Hensel K., Leštinský M., Homola T., and Ráheľ J., Coplanar surface barrier discharge assisted generation of discharges inside the honeycomb monolith, *17th Symposium on Applications of Plasma Processes*, pp. 163–164, 2009.
[37] Höft H., Becker M. M., and Kettlitz M., Impact of gas flow rate on breakdown of filamentary dielectric barrier discharges, *Phys. Plasmas*, Vol. 23 (3), pp. 033504, 2016.
[38] Kim H.-H., Takeuchi N., Teramoto Y., Ogata A., and Abdelaziz A. A., Plasma candle: A new type of scaled-up plasma jet device, *Int. J. Plasma Environ. Sci. Technol*., Vol. 14 (1), pp. e01004, 2020.
[39] Xian Y. B.,Xu, H.T., Lu, X.P., Pei, X.K., Gong W.W., Lu, Y., Liu D.W., and Yang Y., Plasma bullets behavior in a tube covered by a conductor, *Phys. Plasmas*, Vol. 22 (6), pp. 063507, 2015.
[40] Nguyen D. B., Mok Y. S., and Lee W. G., Enhanced atmospheric pressure plasma jet performance by an alternative dielectric barrier discharge configuration, *IEEE Trans. Plasma Sci.*, Vol. 47 (11), pp. 4795–4801, 2019.
[41] Bian X., Meng X., Wang L., MacAlpine J. M. K., Guan Z., and Hui J., Negative corona inception voltages in rod-plane gaps at various air pressures and humidities, *IEEE Trans. Dielectr. Electr. Insul*., Vol. 18 (2), pp. 613–619, 2011.
[42] Bian X., He Z., Zhu J., Pi X., Wan S., and Qi L., Effects of humidity on variation of negative corona-generated space charge in rod to plane electrode, *J. Eng*., Vol. 2019 (16), pp. 2869–2872, 2019.
[43] Ryzko H., Drift velocity of electrons and ions in dry and humid air and in water vapour, *Proc. Phys. Soc*., Vol. 85 (6), pp. 1283–1295, 1965.
[44] Chen J. and Wang P., Effect of relative humidity on electron distribution and ozone production by DC coronas in air, *IEEE Trans. Plasma Sci*., Vol. 33 (2), pp. 808–812, 2005.
[45] Falkenstein Z. and Coogan J. J., Microdischarge behaviour in the silent discharge of nitrogen-oxygen and water-air mixtures, *J. Phys. D. Appl. Phys*., Vol. 30 (5), pp. 817–825, 1997.
[46] Kim H.-H., Teramoto Y., Negishi N., and Ogata A., A multidisciplinary approach to understand the interactions

of nonthermal plasma and catalyst: A review, *Catal. Today*, Vol. 256, pp. 13–22, 2015.
[47] Fan X., Kang S., Li J., and Zhu T., Formation of nitrogen oxides (N_2O, NO, and NO_2) in typical plasma and plasma-catalytic processes for air pollution control, *Water. Air. Soil Pollut*., Vol. 229 (11), pp. 351, 2018.
[48] Zhao G. B., Hu X., Argyle M. D., and Radosz M., N atom radicals and N_2 ($A^3\Sigma_u^+$) found to be responsible for nitrogen oxides conversion in non-thermal nitrogen plasma, *Ind. Eng. Chem. Res*., Vol. 43 (17), pp. 5077–5088, 2004.
[49] Tang X., Wang, J., Yi, H., Zhao, S., Gao, F., Huang, Y., Zhang, R., and Yang, Z., N_2O formation characteristics in dielectric barrier discharge reactor for environmental application: Effect of operating parameters, *Energy and Fuels*, Vol. 31 (12), pp. 13901–13908, 2017.
[50] Abdelaziz A. A., Ishijima T., Osawa N., and Seto T., Quantitative analysis of ozone and nitrogen oxides produced by a low power miniaturized surface dielectric barrier discharge: effect of oxygen content and humidity level, *Plasma Chem. Plasma Process*., Vol. 39 (1), pp. 165–185, 2019.
[51] Kučerová K., Machala Z., and Hensel K., Transient spark discharge generated in various N_2/O_2 gas mixtures: reactive species in the gas and water and their antibacterial effects, *Plasma Chem. Plasma Process*., Vol. 40 (3), pp. 749–773, 2020.
[52] Peyrous R., The Effect of relative humidity on ozone production by corona discharge in oxygen or air - a numerical simulation - Part II: Air, *Ozone Sci. Eng*., Vol. 12 (1), pp. 41–64, 1990.
[53] Pinart J., Smirdec, M., Pinart, M.E., Aaron, J.N., Benmansour, Z., Goldman, M., Goldman, A., Quantitative study of the formation of inorganic chemical species following corona discharge - I. Production of HNO_2 and HNO_3 in a composition-controlled, humid atmosphere, *Atmos. Environ*., Vol. 30 (1), pp. 129–132, 1996.
[54] Zhang X., Lee B. J., Im H. G., and Cha M. S., Ozone production with dielectric barrier discharge: effects of power source and humidity, *IEEE Trans. Plasma Sci.*, Vol. 44 (10), pp. 2288–2296, 2016.
[55] Pekárek S., Effect of polarity on ozone production of DC corona discharge with and without photocatalyst, *19th International Symposium on Plasma Chemistry*, 2009.
[56] Abdel-Salam M., Mizuno A., and Shimizu K., Ozone generation as influenced by gas flow in corona reactors, *J. Phys. D. Appl. Phys*., Vol. 30 (5), pp. 864–870, 1997.
[57] Chen J. and Davidson J. H., Ozone production in the negative DC corona: The dependence of discharge polarity, *Plasma Chem. Plasma Process*., Vol. 23 (3), pp. 501–518, 2003.
[58] Brandvold D. K., Martinez P., and Dogruel D., Polarity dependence of N_2O formation from corona discharge, *Atmos. Environ*., Vol. 23 (9), pp. 1881–1883, 1989.
[59] Chen J. and Davidson J. H., Ozone production in the positive DC corona discharge: model and comparison to experiments, *Plasma Chem. Plasma Process*., Vol. 22 (4), pp. 495–522, 2002.
[60] Kim H.-H., Nonthermal plasma processing for air-pollution control: A historical review, current issues, and future prospects, *Plasma Process. Polym*., Vol. 1 (2), pp. 91–110, 2004.